Ferroelectricity and Giant Magnetocapacitance in Perovskite Rare-Earth Manganites

T. Goto,[1] T. Kimura,[2] G. Lawes,[2] A. P. Ramirez,[3] and Y. Tokura[1,4]

[1]*Department of Applied Physics, University of Tokyo, Tokyo 113-8656, Japan*
[2]*Los Alamos National Laboratory, Los Alamos, New Mexico 87545, USA*
[3]*Bell Laboratories, Lucent Technologies, 600 Mountain Avenue, Murray Hill, New Jersey 07974, USA*
[4]*Spin Superstructure Project, ERATO, Japan Science and Technology Agency, Tsukuba 305-8562, Japan*

(Received 30 November 2003; published 22 June 2004)

The relationships among magnetism, lattice modulation, and dielectric properties have been investigated for $R\mathrm{MnO_3}$ (R = Eu, Gd, Tb, and Dy). These compounds show a transition to an incommensurate lattice structure below their Néel temperature, and subsequently undergo an incommensurate-commensurate (IC-C) phase transition. For $\mathrm{TbMnO_3}$ and $\mathrm{DyMnO_3}$ it was found that the IC-C transition is accompanied by a ferroelectric transition, associated with a lattice modulation in the C phase. $\mathrm{DyMnO_3}$ shows a gigantic magnetocapacitance with a change of dielectric constant up to $\Delta\varepsilon/\varepsilon \sim 500\%$.

DOI: 10.1103/PhysRevLett.92.257201 PACS numbers: 75.47.Lx, 64.70.Rh, 75.80.+q

In the past several years there has been a revival of interest in understanding magnetic ferroelectrics [1–3] because of their potential in novel magnetoelectric and magneto-optical devices. Most of the recent studies, however, revisit conventional magnetic ferroelectrics, as listed in a review [4] by Smolenskii and Chupis in 1982. The recent observation of large magnetoelectric and magnetocapacitive effects in $\mathrm{TbMnO_3}$ provides a novel approach to the mutual control of magnetization and electric polarization in magnetic ferroelectrics [5]. $\mathrm{TbMnO_3}$ has the orthorhombically distorted perovskite structure (space group *Pbnm*) at room temperature, and shows an incommensurate (IC) lattice modulation at the Néel temperature ($T_\mathrm{N} \sim 41$ K) for sinusoidal antiferromagnetic (AF) ordering. At lower temperatures, ferroelectric order develops at the incommensurate-commensurate (or lock-in) transition. This close relationship between lattice modulation and ferroelectricity is common to so-called "improper ferroelectrics" such as $\mathrm{K_2SeO_4}$ and $\mathrm{RbZnCl_4}$ [6,7]. Here, the lattice modulation in $\mathrm{TbMnO_3}$ can be regarded as a second harmonic of the sinusoidal AF spin structure [5]. It is likely, therefore, that the ferroelectricity in $\mathrm{TbMnO_3}$ originates in magnetic interactions, through lattice modulations. Supporting this view of $\mathrm{TbMnO_3}$ is the novel phenomenon, which we call "magnetic-field-induced electric polarization flop," where the direction of ferroelectric polarization can be switched from the c to the a axis by the application of magnetic field [5].

To elucidate the relationship between ferroelectricity and magnetoelastically induced lattice modulation in a broader range of magnetic ferroelectrics, we report in this Letter an investigation of the electric properties of single crystals of the perovskite rare-earth manganites $R\mathrm{MnO_3}$ (R = Eu, Gd, Tb, and Dy). Since the lattice modulation in $R\mathrm{MnO_3}$ is strongly dependent on the ionic radius of R (r_R) [8], this systematic study enables us to clarify the origins of the ferroelectricity and the magnetic-field-induced electric polarization flop in these systems. In the course of this study, we discovered giant magnetocapacitance in one of these compounds, $\mathrm{DyMnO_3}$.

First, we briefly review the magnetic phase diagram of orthorhombic $R\mathrm{MnO_3}$ (R = rare earth) as a function of Mn-O-Mn bond angle ϕ (or r_R) [8–11]. As displayed in Fig. 1, the decrease of ϕ suppresses layer-type (A-type) AF order (left lower inset) among the Mn spins. Alternatively, sinusoidal AF order appears at intermediate ϕ (R = Tb and Dy), and then zigzag-type (E-type) AF order (right lower inset) in R = Ho. Recently, the magnetic phase diagram of $R\mathrm{MnO_3}$ was explained in terms of spin frustration caused by the combination of $\mathrm{GdFeO_3}$-type distortion and staggered orbital order [8]. In accord with the modulated magnetic structures, magnetoelastically induced lattice modulations appear in small-r_R compounds. We show in the upper left inset of Fig. 1 a diffraction feature in the reciprocal-space $(0kl)$ zone. The Bragg peaks of the *Pbnm* orthorhombic structure are shown as open circles. Satellites of the Bragg peaks with modulation wave vector $(0, \delta_m, 1)$ are magnetic (crosses), and those of $(0, \delta_l, 0)$ with $\delta_l \approx 2\delta_m$ are crystallographic (closed circles). The upper right inset of Fig. 1 displays the temperature dependence of wave number (δ_l or $2\delta_m$) in $R\mathrm{MnO_3}$ with smaller r_R. As clearly seen in the inset, these systems undergo a lock-in transition at a temperature (T_lock) below T_N as indicated by arrows.

Single crystals of $R\mathrm{MnO_3}$ (R = Eu, Gd, Tb, and Dy) were grown by the floating zone method. The crystals were oriented using Laue XRD patterns, and cut into thin plates with the widest faces perpendicular to the crystallographic principal axes. Ag electrodes were then vacuum deposited onto these faces. The dielectric constant ε was measured over a range of frequencies using an LCR meter. The temperature (T) dependence of the electric polarization P was obtained by measurements of the

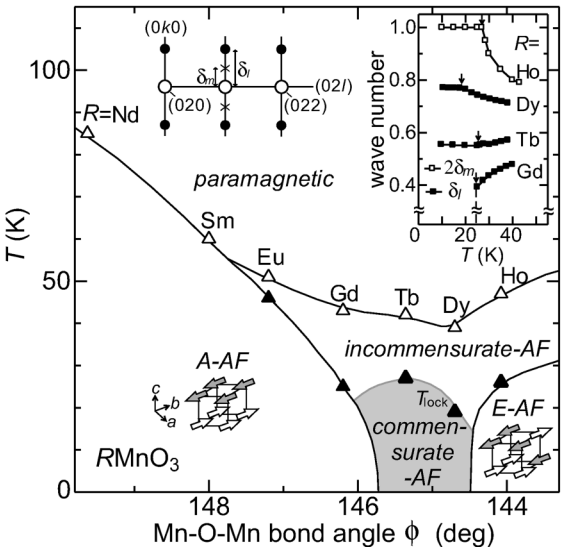

FIG. 1. Magnetic phase diagram for $R\mathrm{MnO_3}$ as a function of Mn-O-Mn bond angle ϕ. Open and closed triangles denote the Néel and lock-in transition temperatures, respectively. Left upper inset: Schematic view of the reciprocal space at a phase with modulated magnetic and crystallographic structure. Open and closed circles represent nuclear Bragg and superlattice reflections, respectively. Crosses give locations of magnetic scattering. Right upper inset: Temperature profiles of the wave numbers of modulated crystallographic (δ_l) or magnetic (δ_m) structures. The arrows indicate the lock-in transition temperatures. Left and right lower insets show schematic illustrations of the *A*-type and the *E*-type AF structures, respectively. The commensurate AF state (gray area) was proved to be ferroelectric by the present study.

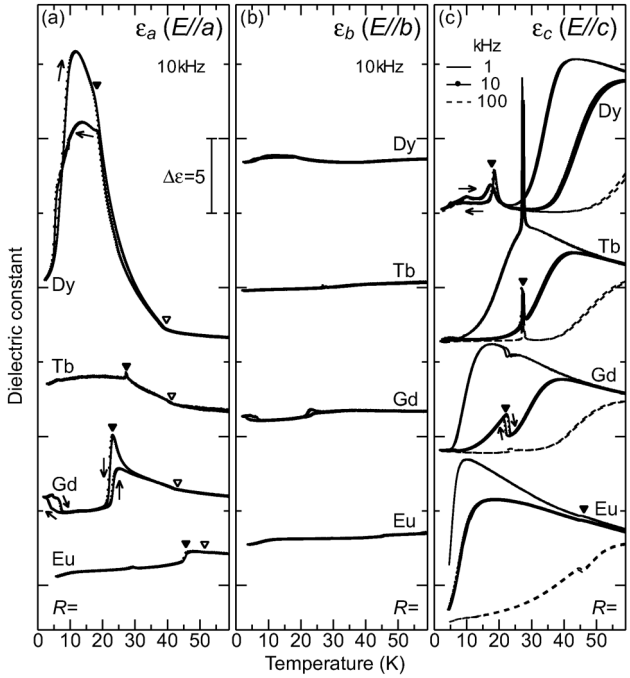

FIG. 2. Temperature dependence of dielectric constant along the *a* (a), *b* (b), and *c* axes (c) for single crystals of $R\mathrm{MnO_3}$ (R = Eu, Gd, Tb, and Dy). The closed and open inverted triangles indicate dielectric anomalies at T_{lock} and T_{N}, respectively. The respective data are vertically offset for clear comparison. Absolute values of ε were 15–35 at 60 K.

pyroelectric current with increasing T, after poling the crystals (~2 kV/cm) while cooling from a temperature above T_{N}.

We display in Fig. 2 the T dependence of ε with the electric field E along the a, b, and c axes for $R\mathrm{MnO_3}$. The T profiles of ε are highly anisotropic in all compounds. ε_a ($E \parallel a$) and ε_b ($E \parallel b$) show little frequency dependence between 0.1 and 100 kHz. Hence, we show only 10 kHz data for ε_a and ε_b in Figs. 2(a) and 2(b). By contrast, ε_c ($E \parallel c$) exhibits significant frequency dependence [Fig. 2(c)], which will be discussed later. Although ε_b shows little T dependence, ε_a and ε_c exhibit sharp anomalies that are associated with the evolution of modulated magnetic and crystallographic structure. Except for $\mathrm{EuMnO_3}$, ε_a shows a steep increase at T_{N} (indicated by open inverted triangles) toward lower temperatures. In $\mathrm{DyMnO_3}$, ε_a increases drastically as T approaches T_{lock} (indicated by closed inverted triangles). With further decreasing T, in $\mathrm{EuMnO_3}$ and $\mathrm{GdMnO_3}$ with nonmodulated crystallographic structure (i.e., $\delta_l = 0$), ε_a shows a sudden drop at T_{lock}. In the case of $\mathrm{TbMnO_3}$ and $\mathrm{DyMnO_3}$ with modulated structures (i.e., $\delta_l \neq$ integer), ε_a does not show a significant drop at T_{lock}, but becomes weakly T dependent below T_{lock}. In ε_c, no dielectric anomaly appears at T_{N} for any of the compounds. At T_{lock}, however, pronounced peak structures in ε_c are evident in $\mathrm{TbMnO_3}$ and $\mathrm{DyMnO_3}$, and also a sharp change in ε_c appears in $\mathrm{GdMnO_3}$ and $\mathrm{EuMnO_3}$. Incidentally, we also observed dielectric anomalies around the magnetic ordering temperature of the R moment [$T_{\mathrm{N}}(R) < 10$ K] [12], which suggests the existence of further magnetoelastically induced lattice deformation.

It should also be noted that a distinct dielectric dispersion is observed only in ε_c over a rather wide T range for all of the crystals, as displayed in Fig. 2(c). Detailed measurements at different temperatures revealed that the frequency ($\omega/2\pi$) dependence of ε_c obeys a Debye model, e.g., can be described by a single relaxation time τ [13]. Above T_{N}, $\ln(T\tau)$ vs $1/T$ plot shows a linear relation with an activation energy of 16, 17, and 25 meV for R = Gd, Tb, and Dy, respectively. However, a non-Arrhenius regime appears below T_{N}. These results may be related to dynamics of localized carriers coupled with lattice that is affected by magnetic ordering.

To clarify the origin of the observed dielectric anomalies, we measured P. The magnitude of P along the a axis (P_a) and the b axis (P_b) was negligibly small for all the compounds in zero magnetic field. By contrast, a characteristic R dependence was observed in P_c. We show in Fig. 3 the T dependence of P_c. Although a substantial signal was not observed in $\mathrm{EuMnO_3}$ and $\mathrm{GdMnO_3}$, a finite spontaneous polarization is evident below T_{lock} in $\mathrm{TbMnO_3}$ and $\mathrm{DyMnO_3}$. Sign reversal of P_c by reversing

E was also confirmed. It is obvious from the comparison with Fig. 1 that the ferroelectric order arises at T_{lock} only in the compounds where the wave number of lattice modulation is fractional ($0 < \delta_l < 1$) at the commensurate (C) phase below T_{lock} [14]. This result confirms that the ferroelectricity in $R\mathrm{MnO_3}$ can be discussed in the framework of improper ferroelectrics [6,7] where P is generated by secondary atomic displacements induced by anharmonic couplings to the primary lattice modulation with nonzero wave vector (i.e., $\delta_l \neq 0$).

Although the accurate knowledge about crystal structure such as atomic position and crystal symmetry in the ferroelectric phase must be obtained by x-ray and/or neutron diffraction measurements, we may have, from the previous [5,8] and present investigations, the following scenario for the origin of ferroelectricity in $\mathrm{TbMnO_3}$ and $\mathrm{DyMnO_3}$. These ferroelectric manganites exhibit the sinusoidal AF order having long wavelength modulation of magnetic coupling along the b axis. Considering strong ϕ dependence on superexchange interactions between nearest neighbor and next-nearest neighbor Mn sites [8], we can expect that the sinusoidal AF order causes modulation of ϕ along the b axis to minimize total energy (i.e., the smallest ϕ at AF-coupled Mn sites across nodes of sinusoid). In addition, it is possible to regard the modulation of ϕ as the very primary order parameter in these improper ferroelectrics. The coupling of the primary order parameter (i.e., modulation of ϕ) with the polarization may induce the ferroelectric ordering in $\mathrm{TbMnO_3}$ and $\mathrm{DyMnO_3}$. Since oxygen ions are not located at centrosymmetric position in the fundamental $Pbnm$ structure, the displacement of oxygen ions can change the space group and produce polar structure.

In ferroelectric $\mathrm{TbMnO_3}$ and $\mathrm{DyMnO_3}$, as shown Fig. 3, anomalies in P_c were observed around $T_{\mathrm{N}}(R)$ ($\lesssim 10$ K, indicated by arrows), which might be related to those in ε and ascribed to the lattice deformations magnetoelastically induced by the ordering of the R moment. For $\mathrm{DyMnO_3}$ in particular, we note the 40% difference in P_c (7 K) obtained after cooling to 2 and 7 K. This implies a strong history dependence for the microscopic process producing ferroelectricity and might bear some relation to the hysteresis in ε shown in Fig. 2.

Finally, we demonstrate gigantic magnetoelectric phenomena observed in $\mathrm{DyMnO_3}$. Figures 4(a) and 4(b) show T variations of P_c and P_a of $\mathrm{DyMnO_3}$ at several magnetic fields along the b axis, respectively. At 1 T, the anomaly in P_c below 10 K disappears and the magnitude of P_c at low T exceeds $\sim 0.2\ \mu\mathrm{C/cm^2}$. However, with further increasing magnetic field (B), P_c is drastically suppressed. Above 4 T, the spontaneous polarization along the c axis totally disappears in a whole T range. By contrast, application of a magnetic field induces a finite P_a [Fig. 4(b)]. These results indicate that the ferroelectric polarization vector is flopped from the direction along the c to the a axis by the application of B, as observed in $\mathrm{TbMnO_3}$ [5]. The

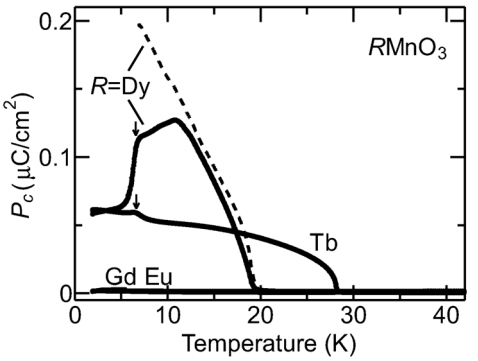

FIG. 3. Temperature profiles of electric polarization along the c axis for crystals of $R\mathrm{MnO_3}$. Solid and dashed lines for $\mathrm{DyMnO_3}$ denote the data obtained after cooling down to 2 and 7 K, respectively. Arrows indicate anomalies around the magnetic ordering temperature of the R moment.

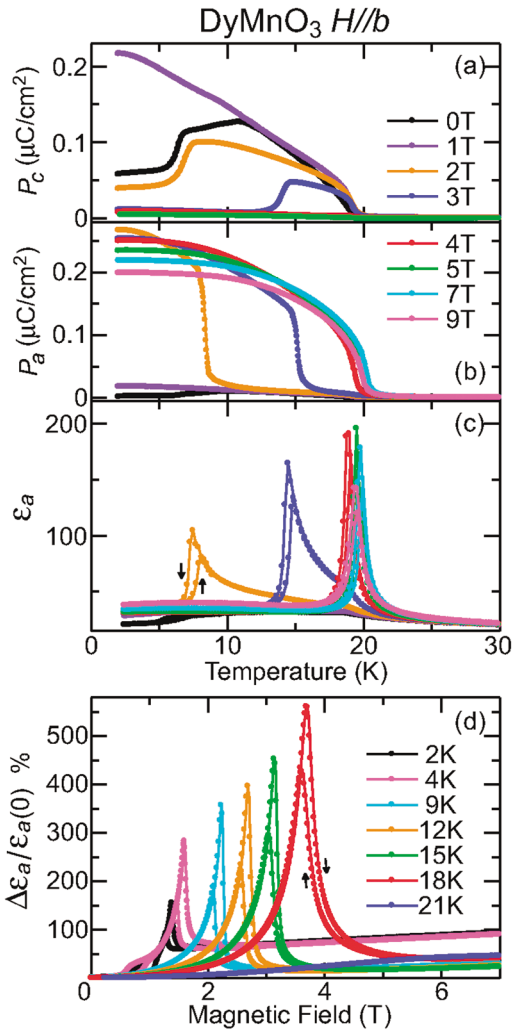

FIG. 4 (color). (a)–(c) Temperature dependence of electric polarization along the c and a axes, and dielectric constant along the a axis at several magnetic fields for crystals of $\mathrm{DyMnO_3}$. (d) Isothermal magnetocapacitance effect at several temperatures with electric field parallel to the a axis. Magnetic field was applied along the b axis.

onset temperature of a finite P_a (T_{flop}) increases with increasing B and is nearly saturated above 4 T. The saturated electric polarization along the a axis gradually decreases with increasing B above 2 T.

Let us mention a possible origin for the flop of electric polarization. We may apply the symmetry-based analysis that explains a sequence of polar phases in some ferroelectric compounds showing an incomplete devil's staircase [15], e.g., $(CH_3)_3NCH_2COO \cdot CaCl_2 \cdot 2H_2O$ (BCCD) [16]. In these compounds, numerous C and IC phases with different modulation wave numbers appear with varying *temperature*. In accordance with the variation of modulation wave number, the direction or the magnitude of polarization changes successively. For instance, in BCCD having the fundamental space group $Pbnm$, the C phases with the modulation wave vector $(\delta, 0, 0)$ [$\delta = 1/4, 2/9, 1/5, \ldots$] exhibit the polarization along the b and c axes, and zero polarization ..., respectively [17,18]. By means of a symmetry analysis, Perez-Mato [16] explains the successive change in polarity of BCCD, and predicts that the polarity of the modulated C phase having wave number $\delta = n/m$ (n and m are integers) depends on the parity of the function δ, i.e., whether n and m are even or odd, as well as on the phase angle of the modulation relative to the unit cell. Such an approach may also be applicable to the magnetic-field-induced polarization flop in $R\text{MnO}_3$. Since the R^{3+} moments also undergo modulated magnetic order [e.g., (0, 0.415, 1) in TbMnO_3 (Ref. [9])], lattice modulation magnetoelastically induced by the R^{3+} magnetic ordering may affect the ferroelectricity. This is clearly signaled as anomalies in ε and P around $T_N(R)$. We speculate that metamagnetic transition of R^{3+} moment induced by B may change the wave number of magnetic and lattice modulations, alter space group, and then switch the ferroelectric polarization vector.

The most striking magnetoelectric phenomenon is observed in the effect of B on ε_a. Figure 4(c) displays T profiles of ε_a in several magnetic fields parallel to the b axis. The application of B causes gigantic enhancement of ε_a below T_{lock} and a sudden change in ε_a at T_{flop}. These are closely correlated with the electric polarization flop, as clearly seen in Figs. 4(a)–4(c). We show in Fig. 4(d) the isothermal magnetocapacitance $\{\Delta\varepsilon_a(B)/\varepsilon_a(0) = [\varepsilon_a(B) - \varepsilon_a(0)]/\varepsilon_a(0)\}$ curves at several temperatures. At each temperature below T_{lock}, $\Delta\varepsilon_a(B)/\varepsilon_a(0)$ diverges with increasing magnetic field then drops suddenly at a magnetic field (B_{flop}). B_{flop} is shifted towards higher B with increasing T. The maximum value of the magnetocapacitance ratio exceeds $\Delta\varepsilon_a(B)/\varepsilon_a(0) \sim 500\%$ at 18 K, which is larger by more than an order of magnitude than those previously reported (e.g. $\sim 7\%$ in EuTiO_3 [19], $\sim 10\%$ in TbMnO_3 [5]).

The data presented here demonstrate the close relation between the electric properties and magnetoelastically induced lattice modulation in perovskite rare-earth manganites $R\text{MnO}_3$. The ferroelectricity was observed only in TbMnO_3 and DyMnO_3 having modulated commensurate phases, and can be explained as the modification of the space group by the lattice modulation in the commensurate phases. In this context, the magnetic-field-induced electric polarization flop may be attributed to the change of modulation wave number by the application of magnetic field. We have also observed an extremely high ratio of magnetocapacitance in DyMnO_3, which implies a path to new magnetoelectric applications.

We thank T. Arima, S. Ishihara, and R. Kajimoto for helpful discussions, and H. Shintani, K. J. McClellan, J. C. Lashley, and J. L. Sarrao for help with sample preparation. This work was in part supported by KAKENHI from the MEXT, Japan and U.S. DOE.

[1] Z. J. Huang *et al.*, Phys. Rev. B **56**, 2623 (1997).
[2] N. A. Hill, J. Phys. Chem. B **104**, 6694 (2000).
[3] M. Fiebig *et al.*, Nature (London) **419**, 818 (2002).
[4] G. A. Smolenskii and I. E. Chupis, Usp. Fiz. Nauk **137**, 415 (1982) [Sov. Phys. Usp. **25**, 475 (1982)].
[5] T. Kimura *et al.*, Nature (London) **426**, 55 (2003).
[6] A. P. Levanyuk and D. G. Shannikov, Usp. Fiz. Nauk **112**, 561 (1974) [Sov. Phys. Usp. **17**, 1999 (1974)].
[7] R. Blinc and A. P. Levanyuk, *Incommensurate Phases in Dielectrics 1. Fundamentals* (North-Holland, Amsterdam, 1986).
[8] T. Kimura *et al.*, Phys. Rev. B **68**, 060403(R) (2003).
[9] S. Quezel *et al.*, Physica (Amsterdam) **86–88B**, 916 (1977).
[10] A. Munoz *et al.*, Inorg. Chem. **40**, 1020 (2001).
[11] J. A. Alonso *et al.*, Inorg. Chem. **39**, 917 (2000).
[12] There is no f moment in EuMnO_3 where Eu^{3+} has no total angular momentum.
[13] P. Debye, *Polar Molecules* (Chemical Catalogue Company, New York, 1929); $\varepsilon(\omega) = \varepsilon(\infty) + [\varepsilon(0) - \varepsilon(\infty)]/[1 + \omega^2\tau^2]$, where $\varepsilon(\infty)$ and $\varepsilon(0)$ are dielectric constants for high and low frequency limits, respectively. τ represents the relaxation time.
[14] In HoMnO_3 with $\delta_m = 1/2$ below T_{lock}, magnetoelastically induced lattice modulation has not yet been observed because of difficulty in preparing single-crystal samples. However, expected wave vector (0, 1, 0) for the lattice modulation may change the extinction rules. The appearance of $(0k0)$ [k = odd] reflections is consistent with the space group $P2_1/n$, which is the same as that in YNiO_3 [J. A. Alonso *et al.*, Phys. Rev. Lett. **82**, 3871 (1999)], and does not allow spontaneous polarization.
[15] P. Bak, Rep. Prog. Phys. **45**, 587 (1982).
[16] J. M. Perez-Mato, Solid State Commun. **67**, 1145 (1988).
[17] W. Brill, W. Schildkamp, and J. Spilker, Z. Kristallogr. **172**, 281 (1985); W. Brill and K. H. Ehses, Jpn. J. Appl. Phys. **24**, Suppl. 24-2, 826 (1985).
[18] H.-G. Unruh *et al.*, Solid State Commun. **70**, 403 (1989).
[19] T. Katsufuji and H. Takagi, Phys. Rev. B **64**, 054415 (2001).